Pharm Res (2014) 31:992–1001
DOI 10.1007/s11095-013-1221-2

RESEARCH PAPER

Thermodynamic and Fluorescence Analyses to Determine Mechanisms of IgG1 Stabilization and Destabilization by Arginine

Masakazu Fukuda • Daisuke Kameoka • Takuya Torizawa • Satoshi Saitoh • Masaya Yasutake • Yoshimi Imaeda • Akiko Koga • Akihiko Mizutani

Received: 11 June 2013 / Accepted: 30 September 2013 / Published online: 28 November 2013

ABSTRACT

Purpose To investigate mechanisms governing the stabilization and destabilization of immunoglobulin (IgG1) by arginine (Arg).

Methods The effects of Arg on the aggregation/degradation, thermodynamic stability, hydrophobicity, and aromatic residues of IgG1 were respectively investigated by size-exclusion chromatography, differential scanning calorimetry, probe fluorescence, and intrinsic fluorescence.

Results Arg monohydrochloride (Arg–HCl) suppressed IgG1 aggregation at near-neutral pH, but facilitated aggregation and degradation at acidic pH or at high storage temperature. Equimolar mixtures of Arg and aspartic acid (Asp) or glutamic acid (Glu) suppressed aggregation without facilitating degradation even at high temperature. Arg–HCl decreased the thermodynamic stability of IgG1 by enthalpic loss, which was counteracted by using Asp or Glu as a counterion for Arg. The suppression of aggregation by Arg–HCl was well correlated with the decrease in hydrophobicity of IgG1. The intrinsic fluorescence of IgG1 was unaffected by Arg–HCl.

Conclusions Suppression of IgG1 aggregation can be attributed to the interaction between Arg and hydrophobic residues; on the other hand, facilitation of aggregation and degradation is presumably due to the interaction between Arg and some acidic residues, which could be competitively inhibited by simultaneously adding either Asp or Glu.

M. Fukuda (✉) • D. Kameoka • M. Yasutake • Y. Imaeda • A. Mizutani
Product Engineering Department, Chugai Pharmaceutical Co., Ltd.
5-5-1 Ukima, Kita-ku, Tokyo 115-8543, Japan
e-mail: fukuda.masakazu76@chugai-pharm.co.jp

S. Saitoh • A. Koga
CMC Development Department, Chugai Pharmaceutical Co., Ltd.
5-5-1 Ukima, Kita-ku, Tokyo 115-8543, Japan

T. Torizawa
Discovery Research Department, Chugai Pharmaceutical Co., Ltd.
200 Kajiwara, Kamakura City, Kanagawa 247-8530, Japan

KEY WORDS aggregation · arginine · degradation · DSC · IgG

ABBREVIATIONS

Arg–Asp	Arginine–aspartic acid mixture
Arg–Glu	Arginine–glutamic acid mixture
Arg–HCl	Arginine monohydrochloride
Bis-ANS	4,4′-dianilino-1,1′-binaphthyl-5,5′-disulfonic acid dipotassium salt
C_p	Molar heat capacity at constant pressure
DSC	Differential scanning calorimetry
SEC	Size-exclusion chromatography

INTRODUCTION

Protein aggregation is a critical issue for the biopharmaceutical industry because it leads to loss of biological activity during long-term storage and could also increase the risk of unfavorable immunogenic responses after administration (1). Arginine (Arg) is a commonly used formulation additive to suppress the aggregation of biopharmaceuticals. It is well established that Arg reduces protein–protein and protein–surface interactions; therefore, Arg is used in various biotechnological applications, e.g., for improving the refolding efficiency of recombinant proteins (2,3), for solubilization of proteins from loose "flocculate-type" inclusion bodies (4,5), for elution of antibodies from protein-A affinity resins (6,7), for improving separation and recovery of proteins in various chromatographic techniques (8), and for concentrating protein solutions used in structural biological studies (9–11).

Several mechanisms by which Arg suppresses protein aggregation have been proposed. Tsumoto *et al.* reported that guanidine remarkably increases the solubility of tryptophan presumably due to the cation–π interaction between the guanidinium group of guanidine and the aromatic ring of tryptophan (12). In that report it is suggested that, similarly

to the suppression of protein aggregation by guanidine, the suppression of protein aggregation by Arg is attributed to the cation–π interaction between the guanidinium group of Arg and aromatic residues. Indeed, Arakawa *et al.* and Ghosh *et al.* have reported that Arg remarkably increases the solubility of aromatic amino acids (13,14). Furthermore, Ito *et al.* have recently demonstrated by using high-resolution X-ray analysis of Arg–lysozyme complexes that Arg molecules bind to aromatic residues on the lysozyme surface via the cation–π interaction (15).

On the other hand, by using mass spectroscopic and light scattering analyses, Das *et al.* detected molecular clusters of Arg in solutions and proposed that due to the alignment of Arg's three methylene groups these molecular clusters display a hydrophobic surface that masks the hydrophobic regions of proteins and inhibits protein aggregation (16). Shukla *et al.* performed molecular dynamics simulations of aqueous Arg solutions containing α–chymotrypsinogen A and melittin, and revealed that Arg self-associates with head-to-tail hydrogen bonding and interacts with aromatic residues via the cation–π interaction and with charged residues via salt-bridge formation (17). In that report, Shukla *et al.* propose that the self-interactions of Arg and the Arg–protein interactions lead to the formation of Arg clusters at the surface of proteins, which, due to their size, crowd out the protein–protein interaction. They also suggest that interactions between Arg and aromatic residues alone cannot account for the suppression of aggregation by Arg because the number of Arg molecules bound to aromatic residues would be a small fraction of the total number of Arg molecules associated with proteins.

Arg is well known to suppress aggregation of many proteins; however, Shah *et al.* have recently reported that Arg can enhance heat-induced aggregation of several proteins (e.g., BSA and β-lactoglobulin), indicating that Arg is not a universal suppressor of aggregation and has potentially negative effects on protein stability (18). In that report it was suggested on the basis of experimental and computational results that the guanidinium group of Arg facilitates protein aggregation by hydrogen-bond–base bridging interactions with the acidic residues of proteins, whereas binding of the guanidinium group to aromatic residues contributes to suppression of aggregation.

Thus, several hypotheses have been proposed to explain the mechanisms by which Arg suppresses and facilitates protein aggregation, but the exact mechanisms are still not fully understood. Elucidation of the comprehensive mechanisms governing protein stabilization and destabilization by Arg will potentially lead to the development of new additives that are similar to Arg, but more effective at suppressing protein aggregation. To clarify this issue, we investigated the effects of Arg on the aggregation and degradation of immunoglobulin G (IgG1) under various solution conditions differing in Arg concentration, counterions of Arg, and pH values. Subsequently, by using differential scanning calorimetry (DSC) and probe fluorescence analysis, respectively, we examined the effects of Arg on the thermodynamic stability and hydrophobicity of IgG1. We also investigated the interaction between Arg and aromatic residues of IgG1 by examining the intrinsic fluorescence of IgG1. These results provided new insights into the mechanisms governing the stabilization and destabilization of proteins by Arg.

MATERIALS AND METHODS

Materials

The IgG1 used in this study was a humanized IgG1 monoclonal antibody to human interleukin-6 receptor manufactured and provided by Chugai Pharmaceuticals (Tokyo, Japan). Arg, Arg monohydrochloride (Arg–HCl), aspartic acid (Asp), and glutamic acid (Glu) were purchased from Ajinomoto Healthy Supply (Tokyo, Japan). 4,4′-Dianilino-1,1′-binaphthyl-5,5′-disulfonic acid dipotassium salt (bis-ANS) was purchased from Molecular Probes (Eugene, OR). The TSK-gel G3000SW$_{XL}$ column was purchased from Tosoh (Tokyo, Japan). All other chemicals were obtained from Wako Pure Chemicals (Osaka, Japan). The IgG1 was formulated at a concentration of 100 mg/mL with different Arg concentrations (i.e., 0, 100, 300, or 500 mM), different counterions of Arg (i.e., Cl, Asp, or Glu), and different pH values (i.e., 4.5, 5.2, or 6.0). The protein concentration of the samples was determined using UV absorbance at 280 nm. Blank solutions—the same buffer solutions but without the IgG1—corresponding to each IgG1 solution were also prepared.

Size-Exclusion Chromatography (SEC)

The aggregates, monomer, and degradate of the IgG1 were separated by size-exclusion chromatography (SEC), using a Waters Alliance HPLC system (Milford, MA) equipped with a TSK-gel G3000SW$_{XL}$ column. A running buffer of 50 mM phosphate, 300 mM NaCl, 0.5 mg/mL NaN_3, pH 7.0 was used at a flow rate of 0.5 mL/min. Heat-treated and non-heat-treated IgG1 solutions were diluted to 1 mg/mL with running buffer and applied to the HPLC system. The heat treatments were 4 weeks storage at 40°C or 1 week storage at 60°C. The elution profiles were detected by UV absorbance at 280 nm and normalized by the monomer peak intensity. The contents of aggregates and degradate were calculated from the area under each peak. The increases in content of aggregates (Δaggregates (%)) and degradate (Δdegradate (%)) that occurred during heat treatments were determined by subtracting the contents of aggregates (0.3%) and degradate (0%) of the non-heat-treated IgG1. For example, 2% of Δaggregates means an increase of aggregates from 0.3% to 2.3%.

Differential Scanning Calorimetry (DSC)

The differential scanning calorimetry (DSC) measurements were performed using a Nano DSC (TA Instruments, New Castle, DE) equipped with capillary cells. Each IgG1 solution was diluted to 1 mg/mL with the corresponding blank solution. DSC scans were performed at a rate of 1°C/min from 30°C to 105°C. Data were analyzed with NanoAnalyze software (TA instruments). Thermograms of each IgG1 solution were corrected by subtracting the thermogram of the corresponding blank solution and normalizing to the IgG1 concentration. The DSC curves were fitted by a two-state model of five independent domains to obtain the thermal denaturation temperature (T_m (°C)) and the enthalpy change (ΔH (kJ/mol)) during thermal denaturation of each domain. Because the change in Gibbs free energy ($\Delta G = \Delta H - T\Delta S$) during thermal denaturation becomes zero at $T = T_m$, the entropy change (ΔS (kJ/mol·K)) during thermal denaturation of each domain was calculated by the following equation using the experimental values of T_m and ΔH.

$$\Delta S = \Delta H/(T_m + 273.15) \quad (1)$$

The changes in T_m, ΔH, and ΔS that occurred by adding Arg were calculated, and are referred to hereafter as ΔT_m, $\Delta\Delta H$, and $\Delta\Delta S$, respectively.

Fluorescence Measurements

Fluorescence measurements were performed with a Shimadzu RF-5300PC spectrofluorometer (Kyoto, Japan). For bis-ANS fluorescence measurements, the heat-treated and non-heat-treated IgG1 solutions were diluted to 3 mg/mL with the corresponding blank solutions, and then bis-ANS solution (1.8 mM bis-ANS in water) was added to the diluted IgG1 solutions to obtain a final concentration of 1 μM bis-ANS. The heat treatment was 4 weeks storage at 40°C. Fluorescence spectra of bis-ANS were recorded from 400 to 650 nm with an excitation wavelength of 385 nm. The bis-ANS fluorescence spectrum of each IgG1 solution was corrected by subtracting the spectrum of the corresponding blank solution. It was confirmed that the bis-ANS spectra in the absence of the IgG1 practically did not change over the range of pH and Arg concentrations investigated in this study. For intrinsic fluorescence measurements, each non-heat-treated IgG1 solution was diluted to 3 mg/mL with the corresponding blank solution. Fluorescence spectra of IgG1 were recorded from 300 to 380 nm with an excitation wavelength of 290 nm. The intrinsic fluorescence spectrum of each IgG1 solution was corrected by subtracting the spectrum of the corresponding blank solution.

RESULTS

Effects of Arg on the Aggregation and Degradation of IgG1

First, the effects of Arg–HCl on the aggregation and degradation of IgG1 were examined at different pH values. The IgG1 solutions were incubated at 40°C for 4 weeks and then analyzed by SEC. Figure 1 shows a representative chromatogram of one of the IgG1 solutions after heat treatment. The peak eluted at about 18 min corresponds to the monomeric IgG1, while the peaks at shorter/longer elution times represent aggregates/degradate, respectively. The peak eluted at about 19.5 min could not be quantified because it overlapped with the monomer peak and could not be successfully separated. We previously reported that the hinge region of IgG1 is subject to hydrolysis (19); therefore, the peaks eluted at about 22.5 and 19.5 min presumably correspond to the Fab fragment and its hydrolyzed counterpart, respectively. At pH 5.2 and 6.0, Arg–HCl suppressed aggregation and the effect reached a plateau at about 500 mM (Fig. 2a). Conversely, at pH 4.5, Arg–HCl facilitated aggregation and the effect was approximately proportional to the concentration of Arg–HCl (Fig. 2a, inset). Arg–HCl did not affect the degradation at pH 6.0, but notably facilitated degradation at lower pH (Fig. 2b).

Next, the effects of Arg counterions were examined at pH 6.0. The IgG1 solutions were incubated at 60°C for 1 week and then analyzed by SEC. Arg–HCl suppressed aggregation at a low concentration (i.e., 100 mM), but facilitated aggregation at higher concentrations (i.e., 300 and 500 mM) (Fig. 3a). Furthermore, Arg–HCl slightly but substantially facilitated degradation. On the other hand, Arg–Asp and Arg–Glu suppressed aggregation (Fig. 3a) without facilitating degradation (Fig. 3b).

Taken together, at 40°C, Arg–HCl suppressed aggregation at near-neutral pH, but facilitated aggregation and degradation at acidic pH. At higher storage temperature (i.e., 60°C), Arg–HCl facilitated aggregation and degradation even at near-neutral pH, whereas Arg–Asp and Arg–Glu suppressed aggregation without facilitating degradation, suggesting that Asp and Glu counteract the potentially disadvantageous effects of Arg: the facilitation of aggregation and degradation.

Thermodynamics of Thermal Denaturation of IgG1

To elucidate the mechanisms behind the complicated effects of Arg on aggregation and degradation, we used DSC to investigate the effects of Arg on the thermodynamic stability of IgG1.

A representative DSC curve of one of the IgG1 solutions is shown in Fig. 4. As previously reported, we can clearly observe three independent domains, which, in order of increasing temperature, are the CH2, CH3, and Fab domains (20).

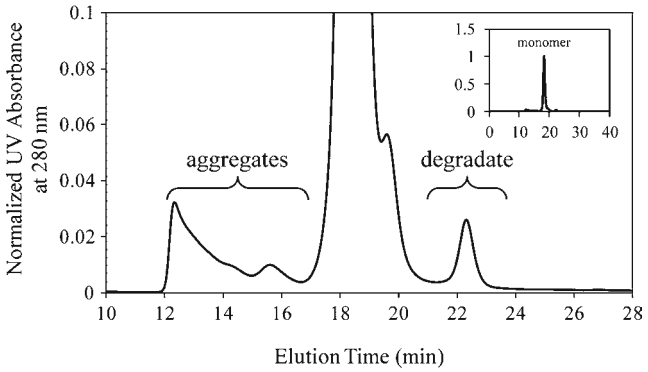

Fig. 1 Representative size-exclusion chromatogram of IgG1 solution at pH 4.5 with 500 mM Arg–HCl after 4 weeks storage at 40°C, showing the magnified peak area of aggregates and degradate. Inset depicts the whole elution profile from 0 to 40 min. For each experiment, heat-treated and non-heat-treated IgG1 solutions (100 mg/mL) were diluted to 1 mg/mL with running buffer and applied to the HPLC system. The elution profiles were detected by UV absorbance at 280 nm and normalized by the monomer peak intensity.

These three domains are spatially separated because the T_m of the Fab domain of IgG1 is extremely high. We have previously reported that the thermal denaturation of the Fab domain is an irreversible process (20); however, in this study, we analyzed the DSC curves of IgG1 assuming that all domains of IgG1 are reversibly denatured via a two-state process. The DSC curves of IgG1 could not be successfully fitted by three or four domains (21), but were well fitted by five domains, which, in order of increasing temperature, are

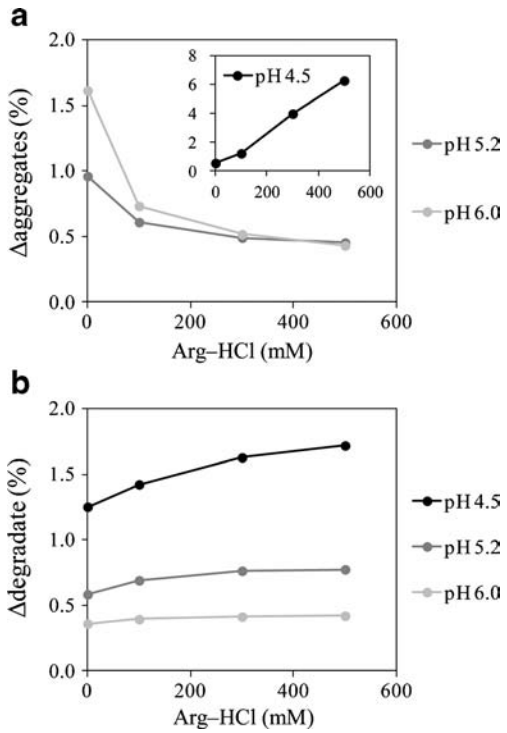

Fig. 2 The increase in aggregates ((**a**) Δaggregates (%)) and degradate ((**b**) Δdegradate (%)) in IgG1 solutions (100 mg/mL) at pH 4.5–6.0 with 0–500 mM Arg–HCl that occurred during 4 weeks storage at 40°C.

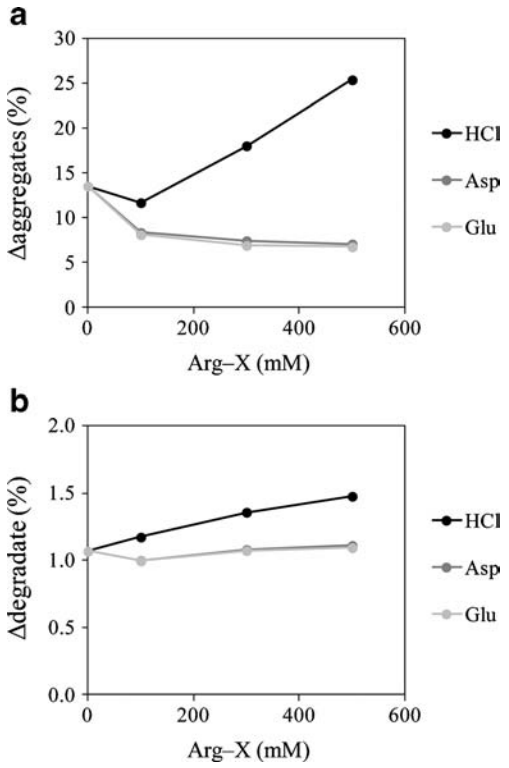

Fig. 3 The increase in aggregates ((**a**) Δaggregates (%)) and degradate ((**b**) Δdegradate (%)) in IgG1 solutions (100 mg/mL) at pH 6.0 with 0–500 mM Arg–X (X = HCl, Asp, or Glu) that occurred during 1 week storage at 60°C.

referred to here as CH2, CH3, Fab[1], Fab[2], and Fab[3], respectively.

First, we examined the effects of Arg–HCl on the thermodynamic parameters at different pH values. Figures 5a, b, and c show the DSC curves of IgG1 solutions at pH 4.5, 5.2, or 6.0 in the absence or presence of Arg–HCl. All DSC curves were deconvoluted into five independent domains, and the values of T_m, ΔH, and ΔS were obtained for each domain. The changes in T_m (ΔT_m), ΔH ($\Delta\Delta H$), and ΔS ($\Delta\Delta S$) that occurred by adding Arg–HCl were calculated and listed in Table I. The values of ΔT_m of each domain were negative at each pH, and the value of ΔT_m progressively decreased with lowering pH, indicating that IgG1 is thermodynamically destabilized by Arg–HCl, especially at lower pH. Both $\Delta\Delta H$ and $\Delta\Delta S$ of each domain were also negative at each pH, indicating that enthalpy–entropy compensation occurred and that thermodynamic destabilization was induced by enthalpic loss, which exceeded entropic gain. Interestingly, Arg–HCl decreased the peak height (molar heat capacity at constant pressure (C_p (kJ/mol)) of Fab domain and the effect reached a plateau at about 500 mM (Fig. 6), where the suppression of aggregation by Arg–HCl also reached a plateau. The decrease in C_p can be interpreted as the enthalpic destabilization of the protein. To examine the relationship between the suppression of aggregation and the enthalpic destabilization, Δaggregation (%) after 4 weeks storage at 40°C was plotted as a function of the

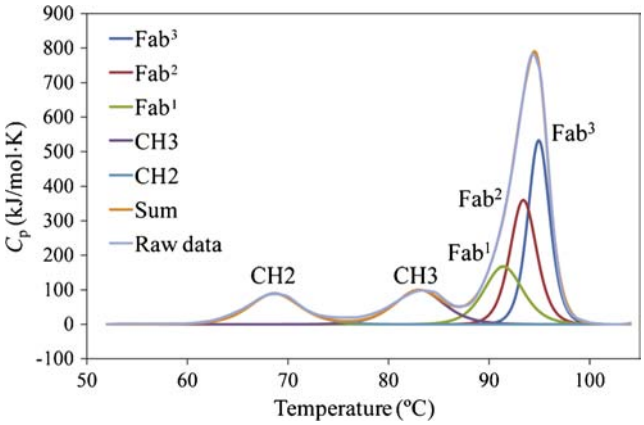

Fig. 4 Representative curve fitting of DSC thermogram of the IgG1 solution at pH 5.2 with 0 mM Arg–HCl. For each experiment, the IgG1 solutions (1 mg/mL) were scanned at a rate of 1 °C/min from 30°C to 105°C. The DSC curves were fitted by a two-state model of five independent domains.

maximum C_p of Fab domain among the IgG1 solutions at pH 6.0 with 0 to 500 mM Arg–HCl (Fig. 8). The suppression of aggregation was loosely correlated with the decrease in the maximum C_p of Fab domain ($R^2 = 0.898$). The maximum C_p of other domains was also decreased by Arg–HCl; however, the change was so small that we could not quantitatively evaluate the correlation with the suppression of aggregation.

Next, the effects of counterions to Arg were examined at pH 6.0. The DSC curve of the IgG1 solution with 500 mM Arg–Asp almost totally overlapped with the DSC curve of the IgG1 solution with 500 mM Arg–Glu (Fig. 5c). The values of ΔT_m, $\Delta\Delta H$, and $\Delta\Delta S$ of each domain are listed in Table II. Similarly to the results with Arg–HCl, both $\Delta\Delta H$ and $\Delta\Delta S$ of each domain were negative for Arg–Asp and Arg–Glu; however, contrary to the results with Arg–HCl, the ΔT_m values of the Fab and CH3 domains were positive and the ΔT_m value of the CH2 domain was practically unaffected by Arg–Asp or Arg–Glu, indicating that Arg–Asp and Arg–Glu thermodynamically stabilized IgG1 by entropic gain, which exceeded enthalpic loss. It is noteworthy that the enthalpic loss of the Fab and CH3 domains by Arg–HCl was substantially counteracted by adding Asp or Glu in place of HCl. The counteracting effect of Asp and Glu was observed especially clearly for the Fab^1 domain (i.e., the $\Delta\Delta H$ values of Arg–HCl, Arg–Asp, and Arg–Glu were -288 ± 19, -160 ± 10, and -142 ± 8 kJ/mol, respectively).

Bis-ANS Fluorescence

Bis-ANS fluorescence measurements were performed to evaluate the effects of Arg on the exposure of hydrophobic regions in the IgG1 at different pH values. Figure 7a and b show the fluorescence spectra of bis-ANS in the non-heat-treated and heat-treated IgG1 solutions with 0 or 500 mM Arg–HCl. Under non-heat treatment condition, Arg–HCl decreased

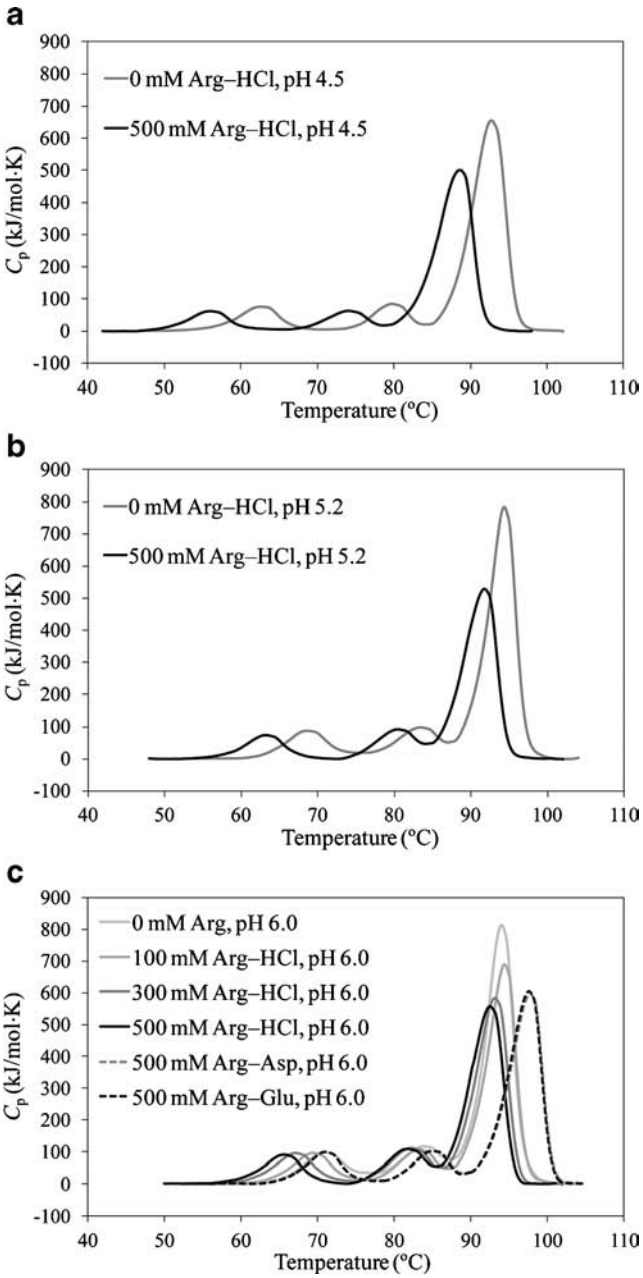

Fig. 5 DSC thermograms of IgG1 solutions (1 mg/mL) under different buffer conditions: (**a**) 0 or 500 mM Arg–HCl, pH 4.5; (**b**) 0 or 500 mM Arg–HCl, pH 5.2; (**c**) 0, 100, 300 or 500 mM Arg–X (X = HCl, Asp, or Glu), pH 6.0.

the fluorescence intensity of bis-ANS without a peak shift at all pH values. Under heat treatment condition, Arg–HCl decreased the fluorescence intensity of bis-ANS without a peak shift at pH 5.2 or 6.0; however, increased the intensity with a blue shift at pH 4.5, the pH at which aggregation and degradation was facilitated by Arg–HCl. The fluorescence intensity of bis-ANS at 500 nm was summarized at Table II.

We also investigated the correlation between Arg concentration and decrease in the hydrophobicity of IgG1. Figure 8a shows the fluorescence spectra of bis-ANS in the non-heat-

Table I Changes in T_m (ΔT_m (°C)), ΔH ($\Delta\Delta H$ (kJ/mol)), and ΔS ($\Delta\Delta S$ (kJ/mol·K)) by Adding 100–500 mM Arg–X (X = HCl, Asp or Glu) at pH 4.5–6.0

pH	Arg concentrations (mM)	Counterions of Arg	Domains	ΔT_m (°C)[a]	$\Delta\Delta H$ (kJ/mol)[a]	$\Delta\Delta S$ (kJ/mol·K)[a, b]
4.5	500	Cl	CH2	−6.5 ± 0.2	−79 ± 8	−0.21 ± 0.02
			CH3	−5.8 ± 0.0	−67 ± 13	−0.17 ± 0.04
			Fab^1	−4.7 ± 0.1	−214 ± 10	−0.56 ± 0.03
			Fab^2	−4.6 ± 0.1	−212 ± 17	−0.54 ± 0.05
			Fab^3	−4.3 ± 0.1	−125 ± 15	−0.30 ± 0.04
5.2	500	Cl	CH2	−5.8 ± 0.2	−51 ± 17	−0.12 ± 0.05
			CH3	−3.0 ± 0.1	−26 ± 9	−0.06 ± 0.02
			Fab^1	−2.8 ± 0.2	−289 ± 14	−0.78 ± 0.04
			Fab^2	−3.4 ± 0.1	−198 ± 31	−0.51 ± 0.09
			Fab^3	−2.7 ± 0.1	−176 ± 21	−0.45 ± 0.06
6.0	100	Cl	CH2	−1.6 ± 0.1	−7 ± 12	−0.01 ± 0.03
			CH3	−0.6 ± 0.1	−23 ± 3	−0.06 ± 0.01
			Fab^1	0.4 ± 0.1	−122 ± 19	−0.34 ± 0.05
			Fab^2	−0.1 ± 0.0	−233 ± 6	−0.64 ± 0.02
			Fab^3	0.1 ± 0.0	−45 ± 7	−0.12 ± 0.02
6.0	300	Cl	CH2	−4.1 ± 0.1	−21 ± 1	−0.04 ± 0.00
			CH3	−1.7 ± 0.1	−19 ± 12	−0.05 ± 0.03
			Fab^1	−0.9 ± 0.2	−231 ± 55	−0.63 ± 0.15
			Fab^2	−1.5 ± 0.1	−298 ± 22	−0.80 ± 0.06
			Fab^3	−1.0 ± 0.1	−160 ± 9	−0.48 ± 0.02
6.0	500	Cl	CH2	−5.6 ± 0.1	−44 ± 7	−0.10 ± 0.02
			CH3	−2.1 ± 0.0	−40 ± 13	−0.10 ± 0.04
			Fab^1	−1.6 ± 0.2	−288 ± 19	−0.78 ± 0.05
			Fab^2	−2.3 ± 0.0	−286 ± 14	−0.76 ± 0.04
			Fab^3	−1.6 ± 0.1	−186 ± 11	−0.49 ± 0.03
6.0	500	Asp	CH2	−0.2 ± 0.0	−12 ± 7	−0.03 ± 0.02
			CH3	1.3 ± 0.1	−33 ± 9	−0.10 ± 0.02
			Fab^1	3.1 ± 0.2	−160 ± 10	−0.45 ± 0.03
			Fab^2	3.0 ± 0.1	−260 ± 12	−0.74 ± 0.03
			Fab^3	3.5 ± 0.0	−115 ± 6	−0.35 ± 0.02
6.0	500	Glu	CH2	−0.1 ± 0.1	−7 ± 2	−0.02 ± 0.01
			CH3	1.2 ± 0.1	−29 ± 9	−0.09 ± 0.02
			Fab^1	3.0 ± 0.2	−142 ± 8	−0.41 ± 0.02
			Fab^2	3.0 ± 0.0	−243 ± 9	−0.69 ± 0.03
			Fab^3	3.5 ± 0.1	−114 ± 5	−0.35 ± 0.01

[a] The data represent the mean ± SD of three experiments

[b] ΔS was obtained from Eq. 1

treated IgG1 solutions at pH 6.0 with 0 to 500 mM Arg–HCl. The hydrophobicity of the IgG1 was decreased by Arg–HCl in a dose-dependent manner, and the effect of Arg–HCl reached a plateau at about 500 mM. The fluorescence intensity of bis-ANS at 500 nm was summarized at Table III. To relate the two effects of Arg–HCl on IgG1 (i.e., suppressing aggregation and decreasing hydrophobicity), Δaggregation (%) after 4 weeks storage at 40°C was plotted as a function of the fluorescence intensity of bis-ANS at 500 nm among the IgG1 solutions at pH 6.0 with 0 to 500 mM Arg–HCl (Fig. 8b). The suppression of aggregation by Arg was strongly correlated with the decrease in hydrophobicity of the IgG1 ($R^2 = 0.998$).

Intrinsic Fluorescence of IgG1

To clarify whether Arg molecules interact with aromatic residues of IgG1, we evaluated the effects of Arg–HCl on the intrinsic fluorescence of IgG1 at pH 6.0. Figure 9 shows the intrinsic fluorescence spectra of non-heat-

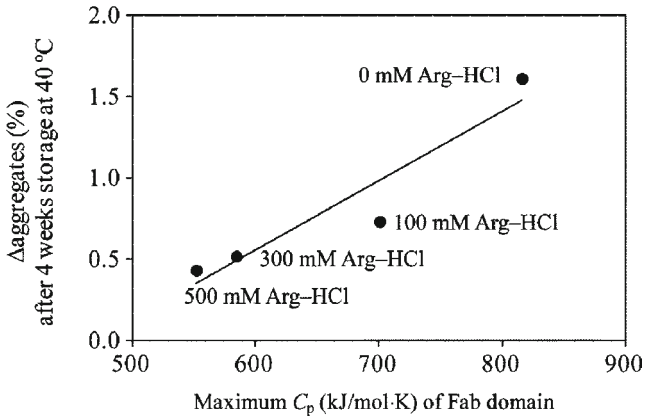

Fig. 6 Correlation between the maximum C_p (kJ/mol) of Fab domain (Fig. 5c) and Δaggregates (%) after 4 weeks storage at 40°C (Fig. 2a) among IgG1 solutions at pH 6.0 with 0–500 mM Arg–HCl.

treated IgG1 solutions with 0 to 500 mM Arg–HCl. The spectra of the IgG1 were practically unaffected by Arg–HCl.

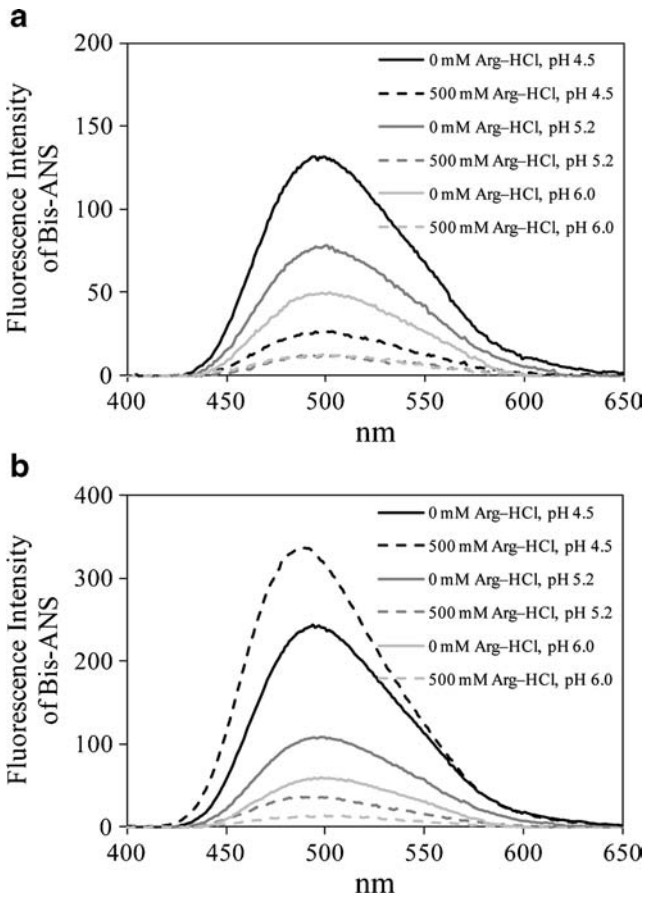

Fig. 7 Fluorescence spectra of bis-ANS in (**a**) non-heat-treated and (**b**) heat-treated IgG1 solutions at pH 4.5–6.0 with 0 or 500 mM Arg–HCl. The heat treatment was 4 weeks storage at 40°C. The concentrations of bis-ANS and the IgG1 were 1 μM and 3 mg/mL, respectively. The excitation/emission slits were set to 3/3 nm.

DISCUSSION

Suppression of Aggregation by Arg

Carpenter *et al.* have reported that the absolute amount of aggregates cannot be determined by SEC method alone due to several reasons (e.g., adsorption to column matrix, inability of large aggregates to pass through the frit and enter the column, etc.) (22). They have proposed that it is essential to confirm the results of SEC with an orthogonal method, especially analytical ultracentrifugation. In the biopharmaceutical industry, the potential inaccurate quantitation by SEC method is a critical issue when determining the absolute amount of aggregates of therapeutic proteins. In this study, however, we assumed that it is sufficient to quantitatively compare the relative (not absolute) amount of aggregates and degradate among each sample for examining the effects of Arg–HCl on the aggregation and degradation of IgG1; therefore, we used SEC method, by which highly reproducible and accurate results can be easily obtained.

The aggregation of IgG1 was suppressed by Arg–HCl at near-neutral pH. The suppression of aggregation was strongly correlated with the decrease in hydrophobicity of the IgG1, demonstrating that the shielding of the hydrophobic regions of the IgG1 was the main driving force for the suppression of aggregation by Arg. Many researchers have suggested that Arg interacts with aromatic residues via the cation–π interaction between the guanidinium group of Arg and aromatic rings (12–15). Ito *et al.* have reported the quenching of intrinsic fluorescence of lysozyme due to the cation–π interaction between Arg and tryptophan residues (15). In reference to this method, we investigated the interaction between Arg and aromatic residues of IgG1 under the same condition as bis-ANS fluorescence experiment. The intrinsic fluorescence spectra of the IgG1 were practically unaffected by Arg–HCl, raising the possibility that Arg scarcely interacts with aromatic residues of IgG1 and the cation–π interaction between Arg and aromatic residues may be not a prerequisite for the suppression of aggregation by Arg. However, we cannot exclude the possibility that there might also be aromatic residues at the surface of the IgG1 which are fully exposed to the solvent in the native, folded state. The fluorescence of solvent-exposed aromatic residues is already quenched by bulk water prior to adding Arg–HCl; therefore, we cannot detect the interaction between Arg–HCl and solvent-exposed aromatic residues by intrinsic fluorescence measurement alone. Further studies are needed to justify whether the cation–π interaction between Arg and aromatic residues is a prerequisite for the suppression of aggregation by Arg or not.

We should also note that the suppression of aggregation was loosely correlated with the decrease in the maximum C_p (kJ/mol) of Fab domain, raising the possibility that the enthalpic destabilization of the IgG1 indirectly plays an

Table II Fluorescence Intensity of bis-ANS at 500 nm in Non-Heat-Treated and Heat-Treated IgG1 Solutions at pH 4.5–6.0 with 0 or 500 mM Arg–HCl

pH	Arg–HCl concentrations (mM)	Fluorescence intensity of bis-ANS at 500 nm[a]	
		before heat treatment	after heat treatment[b]
4.5	0	131 ± 1.3	239 ± 1.9
5.2	0	78 ± 1.3	108 ± 1.2
6.0	0	48 ± 0.9	58 ± 0.7
4.5	500	26 ± 1.0	316 ± 5.4
5.2	500	11 ± 0.9	35 ± 0.6
6.0	500	12 ± 0.3	14 ± 0.4

[a] The data represent the mean ± SD of three experiments. The excitation/emission slits were set to 3/3 nm

[b] The heat treatment was 4 weeks storage at 40°C

important role in the suppression of aggregation by Arg. As discussed below, the positively charged guanidinium group of Arg can perturb the intramolecular hydrogen bonds by interacting with negatively charged acidic residues (i.e., Asp and Glu residues). Arg may be stuck on the protein surface by interacting with acidic residues, where Arg could mask the adjacent exposed hydrophobic residues and reduce hydrophobic protein–protein interactions.

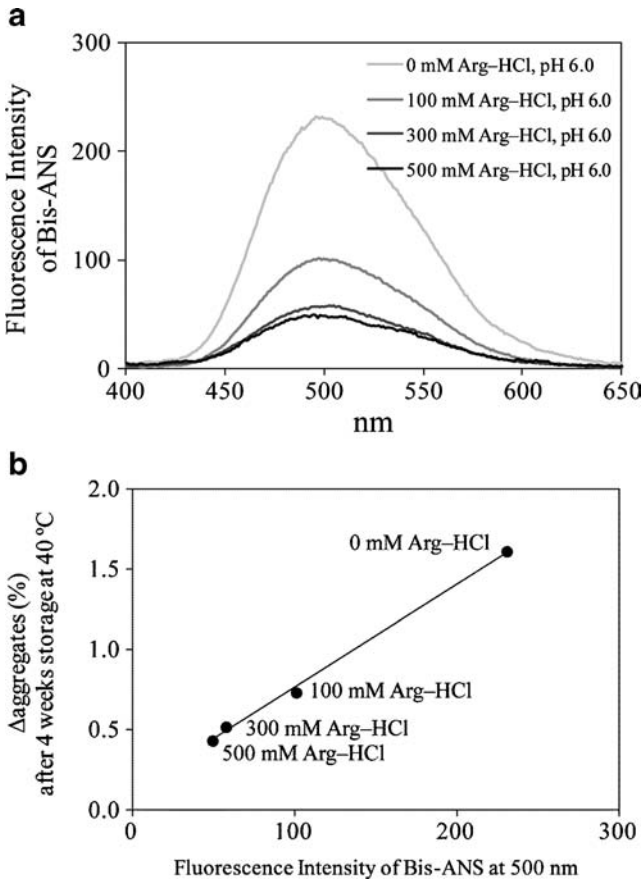

Fig. 8 (**a**) Fluorescence spectra of bis-ANS in non-heat-treated IgG1 solutions at pH 6.0 with 0 to 500 mM Arg–HCl. The concentrations of bis-ANS and the IgG1 were 1 μM and 3 mg/mL, respectively. The excitation/emission slits were set to 3/5 nm. (**b**) Correlation between the fluorescence intensity of bis-ANS at 500 nm (Fig. 8a) and Δaggregates (%) after 4 weeks storage at 40°C (Fig. 2a) among IgG1 solutions at pH 6.0 with 0–500 mM Arg–HCl.

Facilitation of Aggregation and Degradation by Arg

Arg is well known to suppress aggregation of many proteins; however, it has also been reported that Arg facilitates the aggregation of some types of proteins (18). Here, we have demonstrated for the first time that Arg can either suppress or facilitate the aggregation of a particular protein depending on the storage temperature and pH conditions and that Arg also has the potential to facilitate the chemical degradation of proteins. Arg–HCl suppressed the aggregation of IgG1 at near-neutral pH, but facilitated the aggregation and degradation at acidic pH or at high storage temperature. To elucidate the mechanisms by which Arg facilitates aggregation and degradation, we performed DSC analysis. Arg–HCl thermodynamically destabilized the IgG1 by enthalpic loss exceeding entropic gain. At a concentration of 500 mM, Arg–HCl decreased ΔH during thermal denaturation of the Fab, CH2, and CH3 domains by about −300 to −100, −50, and −50 kJ/mol, respectively. The enthalpic loss by Arg would be mainly due to the cleavage of intramolecular hydrogen bonds and salt bridges of the IgG1. On the other hand, the entropic gain by Arg would arise from the increase in conformational flexibility of the IgG1 and the decrease in the hydrophobic hydration (23,24). The conformational destabilization induced by Arg was also detected by bis-ANS fluorescence analysis. Under heat treatment condition, the hydrophobicity of IgG1 was increased by Arg–HCl at pH 4.5, the pH at which the aggregation and degradation was facilitated by Arg–HCl. These results suggest that the facilitation of aggregation by Arg could be attributed to the exposure of hydrophobic regions of the IgG1 to bulk water by the conformational destabilization and that the facilitation of degradation by Arg is probably due to the exposure of the hydrolysis-prone site in the hinge region (19) to bulk water, along with the

Table III Fluorescence Intensity of bis-ANS at 500 nm in Non-Heat-Treated IgG1 Solutions at pH 6.0 with 0–500 mM Arg–HCl

pH	Arg–HCl concentrations (mM)	Fluorescence intensity of bis-ANS at 500 nm[a] before heat treatment
6.0	0	231 ± 1.8
6.0	100	101 ± 0.3
6.0	300	57 ± 1.4
6.0	500	49 ± 0.7

[a] The data represent the mean ± SD of three experiments. The excitation/emission slits were set to 3/5 nm

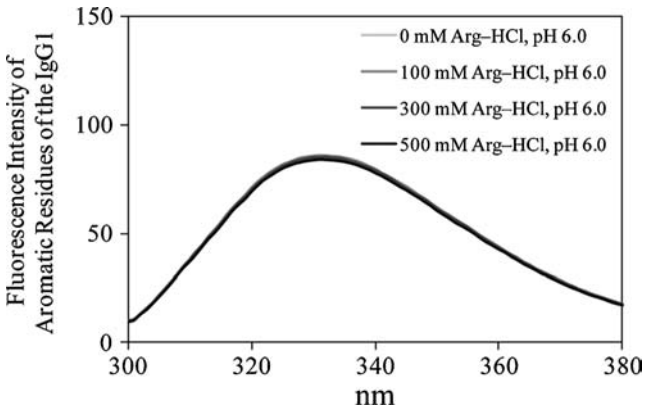

Fig. 9 Intrinsic fluorescence spectra of IgG1 solutions at pH 6.0 with 0–500 mM Arg–HCl. The concentration of the IgG1 was 3 mg/mL. The excitation/emission slits were set to 5/5 nm.

catalytic effect of Arg itself (the guanidinium group of Arg may catalyze the hydrolysis by activating the peptide bonds due to its strong hydrogen bonding property). Arg–HCl facilitated the aggregation and degradation of IgG1 at acidic pH or at high storage temperature, probably because the conformation of the IgG1 is already partially destabilized under these conditions.

Counteraction of the Destabilizing Effects of Arg by Asp and Glu

Golovanov *et al.* showed that the simultaneous addition of Arg and Glu dramatically increased the solubility of poorly soluble proteins by a factor of between 3 and 8 (25). Since then, the synergistic effects of Arg–Glu mixtures on protein solubility have been used to concentrate protein solutions for structural biological studies (9–11). Golovanov *et al.* speculated that the charged side chains of Arg and Glu interact with oppositely charged residues on the surface of the protein, while the aliphatic hydrophobic parts of the side chains of Arg and Glu interact with and cover the adjacent exposed hydrophobic parts of the protein surface. Shukla *et al.* have recently reported that the number of Arg and Glu molecules around the protein is increased by the additional hydrogen bonding interactions between the excipients on the surface of the protein when both excipients are present (26). They proposed that the crowding due to the presence of an enhanced number of Arg and Glu molecules on the protein surface suppresses protein–protein association. Thus, many studies have focused on the synergistic effects of Arg–Glu on protein solubility, but the effects of Arg–Glu on the thermodynamic stability of protein have not been researched.

In this study, we found that Arg–Asp and Arg–Glu are excellent protein stabilizers, which can counteract the potentially disadvantageous effects of Arg–HCl: the facilitation of aggregation and degradation. DSC analysis revealed that, contrary to the effect of Arg–HCl, Arg–Asp and Arg–Glu thermodynamically stabilized IgG1 by entropic gain that exceeded enthalpic loss. The effects of Arg–Asp and Arg–Glu on the aggregation, degradation, and thermodynamic stability of IgG1 were strikingly similar, suggesting that the methylene groups of Asp and Glu do not play a role in the synergistic effects of Asp and Glu. Interestingly, the enthalpic loss of the Fab and CH3 domains by Arg–HCl was substantially counteracted by adding Asp or Glu in place of Cl. One possible explanation for this phenomenon is that Asp and Glu counteract the destabilizing effects of Arg by decreasing the cleavage of intramolecular hydrogen bonds and salt bridges of IgG1 that are induced by Arg. The positively charged guanidinium group of Arg can perturb the intramolecular hydrogen bonds by interacting with negatively charged acidic residues (i.e., Asp and Glu residues), which can form hydrogen bonds and salt bridges with adjacently located positively charged residues. The interactions between Arg and acidic residues, which lead to conformational destabilization, may be inhibited competitively by adding Asp or Glu as a counterion of Arg. It should also be noted that the simultaneous addition of Asp or Glu perfectly inhibited the facilitation of aggregation and degradation by Arg, but could not completely counteract the enthalpic loss by Arg, suggesting that some, but not all, acidic residues induce conformational destabilization by interacting with Arg. As discussed above, other acidic residues may contribute to the suppression of aggregation by interacting with Arg, which could mask the adjacent exposed hydrophobic residues and reduce hydrophobic protein–protein interactions. However, further studies are needed to clarify the molecular mechanisms governing the counteracting effects of Asp and Glu.

CONCLUSION

We investigated the mechanisms by which Arg stabilizes and destabilizes IgG1. Thermodynamic and fluorescence analyses revealed that the suppression of aggregation by Arg can be attributed to the shielding of hydrophobic regions on the IgG1 surface by the interaction between Arg and hydrophobic residues. On the other hand, the facilitation of aggregation and degradation by Arg is presumably due to the conformational destabilization of IgG1 by the interaction between the guanidinium group of Arg and some acidic residues, thereby cleaving intramolecular hydrogen bonds and salt bridges, which could be inhibited competitively by adding Asp or Glu as a counterion of Arg. Other acidic residues may contribute to the suppression of aggregation by interacting with Arg, which could mask the adjacent exposed hydrophobic residues and reduce hydrophobic protein–protein interactions.

ACKNOWLEDGMENTS AND DISCLOSURES

The authors thank Dr. Kohei Tsumoto (Medical Proteomics Laboratory, Institute of Medical Science, The University of Tokyo) for thoughtful discussions. The authors also thank many individuals of our departments for their helpful comments.

REFERENCES

1. Wang W, Singh SK, Li N, Toler MR, King KR, Nema S. Immunogenicity of protein aggregates—concerns and realities. Int J Pharm. 2012;431:1–11.
2. Buchner J, Rudolph R. Renaturation, purification and characterization of recombinant Fab-fragments produced in Escherichia coli. Biotechnology (N Y). 1991;9:157–62.
3. Arora D, Khanna N. Method for increasing the yield of properly folded recombinant human gamma interferon from inclusion bodies. J Biotechnol. 1996;52:127–33.
4. Tsumoto K, Umetsu M, Kumagai I, Ejima D, Arakawa T. Solubilization of active green fluorescent protein from insoluble particles by guanidine and arginine. Biochem Biophys Res Commun. 2003;312:1383–6.
5. Umetsu M, Tsumoto K, Nitta S, Adschiri T, Ejima D, Arakawa T, *et al*. Nondenaturing solubilization of beta2 microglobulin from inclusion bodies by L-arginine. Biochem Biophys Res Commun. 2005;328:189–97.
6. Arakawa T, Philo JS, Tsumoto K, Yumioka R, Ejima D. Elution of antibodies from a Protein-A column by aqueous arginine solutions. Protein Expr Purif. 2004;36:244–8.
7. Ejima D, Yumioka R, Tsumoto K, Arakawa T. Effective elution of antibodies by arginine and arginine derivatives in affinity chromatography. Anal Biochem. 2005;345:250–7.
8. Ejima D, Yumioka R, Arakawa T, Tsumoto K. Arginine as an effective additive in gel permeation chromatography. J Chromatogr A. 2005;1094:49–55.
9. Hautbergue GM, Golovanov AP. Increasing the sensitivity of cryoprobe protein NMR experiments by using the sole low-conductivity arginine glutamate salt. J Magn Reson. 2008;191:335–9.
10. Placzek WJ, Almeida MS, Wüthrich K. NMR structure and functional characterization of a human cancer-related nucleoside triphosphatase. J Mol Biol. 2007;367:788–801.
11. Song J, Zhao KQ, Newman CL, Vinarov DA, Markley JL. Solution structure of human sorting nexin 22. Protein Sci. 2007;16:807–14.
12. Tsumoto K, Umetsu M, Kumagai I, Ejima D, Philo JS, Arakawa T. Role of arginine in protein refolding, solubilization, and purification. Biotechnol Prog. 2004;20:1301–8.
13. Arakawa T, Ejima D, Tsumoto K, Obeyama N, Tanaka Y, Kita Y, *et al*. Suppression of protein interactions by arginine: a proposed mechanism of the arginine effects. Biophys Chem. 2007;127:1–8.
14. Ghosh R, Sharma S, Chattopadhyay K. Effect of arginine on protein aggregation studied by fluorescence correlation spectroscopy and other biophysical methods. Biochemistry. 2009;48:1135–43.
15. Ito L, Shiraki K, Matsuura T, Okumura M, Hasegawa K, Baba S, *et al*. High-resolution X-ray analysis reveals binding of arginine to aromatic residues of lysozyme surface: implication of suppression of protein aggregation by arginine. Protein Eng Des Sel. 2011;24:269–74.
16. Das U, Hariprasad G, Ethayathulla AS, Manral P, Das TK, Pasha S, *et al*. Inhibition of protein aggregation: supramolecular assemblies of arginine hold the key. PLoS One. 2007;2:e1176.
17. Shukla D, Trout BL. Interaction of arginine with proteins and the mechanism by which it inhibits aggregation. J Phys Chem B. 2010;114:13426–38.
18. Shah D, Shaikh RA, Peng X, Rajagopalan R. Effects of arginine on heat-induced aggregation of concentrated protein solutions. Biotechnol Prog. 2011;27:513–20.
19. Kameoka D, Ueda T, Imoto T. Effect of the conformational stability of the CH2 domain on the aggregation and peptide cleavage of a humanized IgG. Appl Biochem Biotechnol. 2011;164:642–54.
20. Kameoka D, Masuzaki E, Ueda T, Imoto T. Effect of buffer species on the unfolding and the aggregation of humanized IgG. J Biochem. 2007;142:383–91.
21. Tischenko VM, Zav'yalov VP, Medgyesi GA, Potekhin SA, Privalov PL. A thermodynamic study of cooperative structures in rabbit immunoglobulin G. Eur J Biochem. 1982;126:517–21.
22. Carpenter JF, Randolph TW, Jiskoot W, Crommelin DJ, Middaugh CR, Winter G. Potential inaccurate quantitation and sizing of protein aggregates by size exclusion chromatography: essential need to use orthogonal methods to assure the quality of therapeutic protein products. J Pharm Sci. 2010;99:2200–8.
23. Lilyestrom WG, Shire SJ, Scherer TM. Influence of the cosolute environment on IgG solution structure analyzed by small-angle X-ray scattering. J Phys Chem B. 2012;116:9611–8.
24. Nakakido M, Tanaka Y, Mitsuhori M, Kudou M, Ejima D, Arakawa T, *et al*. Structure-based analysis reveals hydration changes induced by arginine hydrochloride. Biophys Chem. 2008;137:105–9.
25. Golovanov AP, Hautbergue GM, Wilson SA, Lian LY. A simple method for improving protein solubility and long-term stability. J Am Chem Soc. 2004;126:8933–9.
26. Shukla D, Trout BL. Understanding the synergistic effect of arginine and glutamic acid mixtures on protein solubility. J Phys Chem B. 2011;115:11831–9.